

# Combined Experimental and Computational Study on the Reaction Dynamics of the D1-Silyldiyne(SiD) – Silane (SiH<sub>4</sub>) System

Published as part of *The Journal of Physical Chemistry virtual special issue “Daniel Neumark Festschrift”*.

Zhenghai Yang,<sup>§</sup> Bing-Jian Sun,<sup>§</sup> Chao He, Shane Goettl, Yu-Ting Lin, Agnes H. H. Chang,\* and Ralf I. Kaiser\*

 Cite This: *J. Phys. Chem. A* 2021, 125, 2472–2479

 Read Online

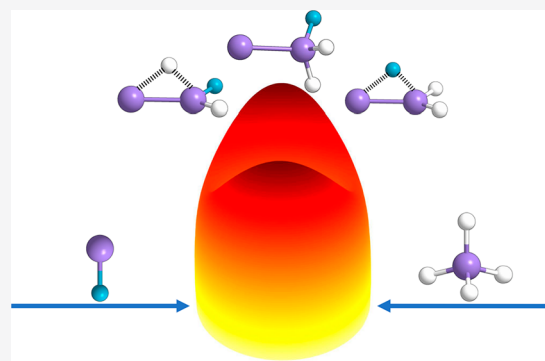
ACCESS |

 Metrics & More

 Article Recommendations

 Supporting Information

**ABSTRACT:** Small silicon hydrides have attracted extensive interest because of their role in the chemical evolution of circumstellar envelopes of evolved carbon stars and applications in surface growth processes and as transients in semiconductor manufacturing. Combined with electronic structure calculations, we demonstrate that monobridged silyldiyne-silylenes [(Si( $\mu$ -D)SiH<sub>2</sub>, Si( $\mu$ -H)SiHD, Si( $\mu$ -H)SiH<sub>2</sub>) and silylsilyldiyne [H<sub>3</sub>SiSi, H<sub>2</sub>DSiSi], which are nearly isoenergetic, can be prepared via molecular hydrogen loss channels in the crossed molecular beam study of the reaction of D1-silyldiyne (SiD; X<sup>2</sup> $\Pi$ ) with silane (SiH<sub>4</sub>; X<sup>1</sup>A<sub>1</sub>) in a crossed molecular beams machine. Compared to the dynamics of the isovalent methylidyne (CH) – methane (CH<sub>4</sub>) system, our study delivers a unique view at the intriguing isomerization processes and reaction dynamics of dinuclear silicon hydride transients, thus contributing to our knowledge on the chemical bonding of silicon hydrides at the molecular level.



## 1. INTRODUCTION

For more than a century, Langmuir’s perception of isovalency<sup>1,2</sup> has been of central importance in the development of fundamental theories of chemical bonding and molecular structure with special devotion attributed to elucidating the similarities and disparities of molecular geometries of the germanium (Ge) and silicon (Si) systems with the second-row carbon (C) system. When comparing the highly reactive and thermally unstable doublet homo- (E<sub>2</sub>H<sub>3</sub>) and heteronuclear (EE’H<sub>3</sub>) trihydrides (E, E’ = C, Si, Ge) (Scheme 1), the distinct bonding chemistry of silicon and germanium versus carbon is reflected. For the C<sub>2</sub>H<sub>3</sub> isomers, the planar vinyl radical (C<sub>2</sub>H<sub>3</sub>; 1; X<sup>2</sup>A’) with a C<sub>s</sub> point group is the most stable isomer,<sup>3–5</sup> with the methylmethylidyne radical (CH<sub>3</sub>C; 2; X<sup>2</sup>A’’) less stable by 205 kJ mol<sup>–1</sup>. However, for the heteronuclear systems, the sequence of stability is reversed with methylsilyldiyne (SiCH<sub>3</sub>; 3; X<sup>2</sup>A’), methylgermyldiyne (GeCH<sub>3</sub>; 7; X<sup>2</sup>A’), and silylgermyldiyne (H<sub>3</sub>SiGe; 11; X<sup>2</sup>A’’) representing global minima with their corresponding vinyl-type counterparts 4, 8, and 12 less stable by 42, 103, and 29 kJ mol<sup>–1</sup>, respectively.<sup>6–8</sup> The distinction can be explained by the increased overlap of the valence s and p orbitals of the carbon atom compared to silicon and germanium.<sup>9</sup> As for Ge<sub>2</sub>H<sub>3</sub>, the global minima within the six Ge<sub>2</sub>H<sub>3</sub> isomers is a vinyl-type planar radical germylgermyldiyne (H<sub>2</sub>GeGeH; 19; X<sup>2</sup>A’), with an unpaired electron that belongs

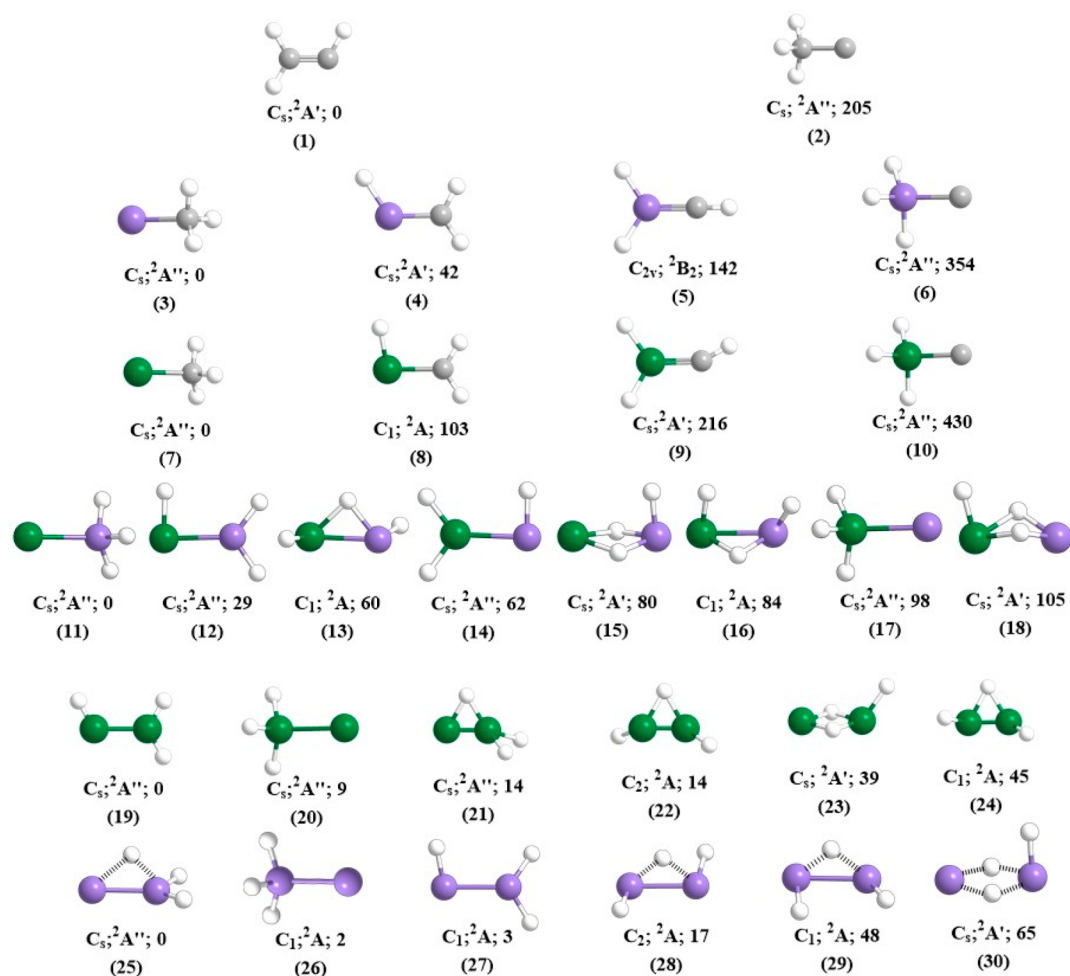
to the  $\pi$ -type orbital perpendicular to the molecular plane.<sup>10–12</sup> In analogy to the vinyl (C<sub>2</sub>H<sub>3</sub>; 1; X<sup>2</sup>A’)–methylmethylidyne (CH<sub>3</sub>C; 2; X<sup>2</sup>A’’) isomer pair,<sup>5</sup> the germylgermyldiyne (GeH<sub>3</sub>Ge; 20; X<sup>2</sup>A’’) isomer is higher in energy than the vinyl-type counterpart 19. Four alternative isomers with higher energy are hydrogen-bridged structures. Among the six Si<sub>2</sub>H<sub>3</sub> isomers (25–30), silylsilyldiyne (H<sub>3</sub>SiSi; 26; X<sup>2</sup>A), vinyl-type disilynyl (H<sub>2</sub>SiSiH; 27; X<sup>2</sup>A), and one monobridged isomer Si(H)SiH<sub>2</sub> (25; X<sup>2</sup>A’’) are nearly isoenergetic. The hydrogen atoms of disilynyl are slightly bent out-of-plane, and thus there is no symmetry at all; this reflects the diverse chemistry of silicon versus carbon and germanium.<sup>13–19</sup> Considering the unusual silicon and germanium bearing mono- and dibridged HGe( $\mu$ -H)SiH (13; X<sup>2</sup>A), Ge( $\mu$ -H<sub>2</sub>)SiH (15; X<sup>2</sup>A’), HGe( $\mu$ -H)SiH (16; X<sup>2</sup>A), HGe( $\mu$ -H<sub>2</sub>)Si (18; X<sup>2</sup>A’), H<sub>2</sub>Ge( $\mu$ -H)Ge (21; X<sup>2</sup>A’), HGe( $\mu$ -H)GeH (22; X<sup>2</sup>A), HGe( $\mu$ -H<sub>2</sub>)Ge (23; X<sup>2</sup>A’), HGe( $\mu$ -H)GeH (24; X<sup>2</sup>A), H<sub>2</sub>Si( $\mu$ -H)Si (25; X<sup>2</sup>A’), HSi( $\mu$ -H)SiH (28; X<sup>2</sup>A), HSi( $\mu$ -H)SiH (29; X<sup>2</sup>A), and HSi( $\mu$ -H<sub>2</sub>)Si (30; X<sup>2</sup>A’) isomers, whose carbon analogue structures

**Received:** December 28, 2020

**Revised:** February 25, 2021

**Published:** March 18, 2021



Scheme 1. Calculated Geometries of Hetero- and Homonuclear Trihydrides  $EE'H_3$  ( $E, E' = C, Si, Ge$ ) along with Their Point Groups, Wave Functions, and Relative Energies ( $\text{kJ mol}^{-1}$ )<sup>a</sup>

<sup>a</sup>Germanium, silicon, carbon, and hydrogen atoms are color coded in green, purple, gray, and white, respectively.

do not exist, the special molecular structure and chemical bonding of heavy main group XIV elements are also reflected.

The  $\text{Si}_2\text{H}_3$  system has received particular attention from the astrochemistry and material science communities, since  $\text{Si}_2\text{H}_3$  isomers may play an important role in elucidating the organo-silicon chemistry in circumstellar envelopes of carbon-rich stars;<sup>20–23</sup> these species are also transients in chemical vapor deposition processes and in semiconductor manufacturing.<sup>24</sup> Ruscic and Berkowitz<sup>25</sup> proposed that successive hydrogen abstraction sequences by atomic fluorine (F) from disilane ( $\text{Si}_2\text{H}_6$ ) lead to nearly isoenergetic isomers of silylsilyldiyne ( $\text{H}_3\text{SiSi}$ ; **26**) and disilenyl ( $\text{H}_2\text{SiSiH}$ ; **27**). Sari et al. recorded the rotational spectrum of disilenyl ( $\text{H}_2\text{SiSiH}$ ; **27**) via Fourier transform microwave spectroscopy.<sup>18</sup> The disilenyl radical ( $\text{H}_2\text{SiSiH}$ ; **27**) along with its deuterated counterpart was also detected via infrared spectroscopy in low temperature (D4)-silane matrices upon irradiation with energetic electrons.<sup>26,27</sup> Furthermore, kinetic experiments in the  $\text{SiH}-\text{SiH}_4$  system revealed the rate constants:  $(4.3 \pm 0.3) \times 10^{-10} \text{ cm}^3 \text{ molecule}^{-1} \text{ s}^{-1}$  at ambient temperature,<sup>28</sup>  $2.8 \times 10^{-10} \text{ cm}^3 \text{ molecule}^{-1} \text{ s}^{-1}$  at ambient temperature,<sup>29</sup> and  $4.8 \times 10^{-11} \text{ cm}^3 \text{ molecule}^{-1} \text{ s}^{-1}$  at 300 K.<sup>30</sup>

To shed information on the dynamics of the formation of  $\text{Si}_2\text{H}_3$  isomers, we conduct a comprehensive crossed molecular

beam investigation of the gas phase reaction of D1-silyldiyne ( $\text{SiD}$ ;  $X^2\Pi$ ) with silane ( $\text{SiH}_4$ ;  $X^1A_1$ ). This system can be classified as a prototype to explore single-collision events between the simplest silicon-bearing radical ( $\text{SiD}$ ) and the simplest saturated silicon bearing molecule ( $\text{SiH}_4$ ) to gain fundamental insights into silicon–silicon bond coupling processes, which is strongly distinct from those of isovalent carbon systems.<sup>31,32</sup> Our experimental data together with electronic structure calculations reveal the formation of monobridged silyldynesilylene [ $\text{Si}(\mu\text{-D})\text{SiH}_2$ ,  $\text{Si}(\mu\text{-H})\text{SiHD}$ ,  $\text{Si}(\mu\text{-H})\text{SiH}_2$ ; **25**] and silylsilyldiyne [ $\text{H}_3\text{SiSi}$ ,  $\text{H}_2\text{DSiSi}$ ; **26**] along with molecular hydrogen and/or hydrogen deuteride via indirect scattering dynamics through the formation of  $\text{Si}_2\text{H}_4\text{D}$  complex(es). These findings reveal that the highly reactive transient  $\text{Si}_2\text{H}_3$  species can be prepared with the universal crossed molecular beam method under controlled experimental conditions.

## 2. METHODS

**2.1. Experimental Section.** The molecular beams experiments of the D1-silyldiyne radical ( $\text{SiD}$ ;  $X^2\Pi$ ) with silane ( $\text{SiH}_4$ ;  $X^1A_1$ ) were performed in a crossed molecular beams apparatus.<sup>31,33,34</sup> The pulsed supersonic D1-silyldiyne beam was produced *in situ* by the laser ablation method using a

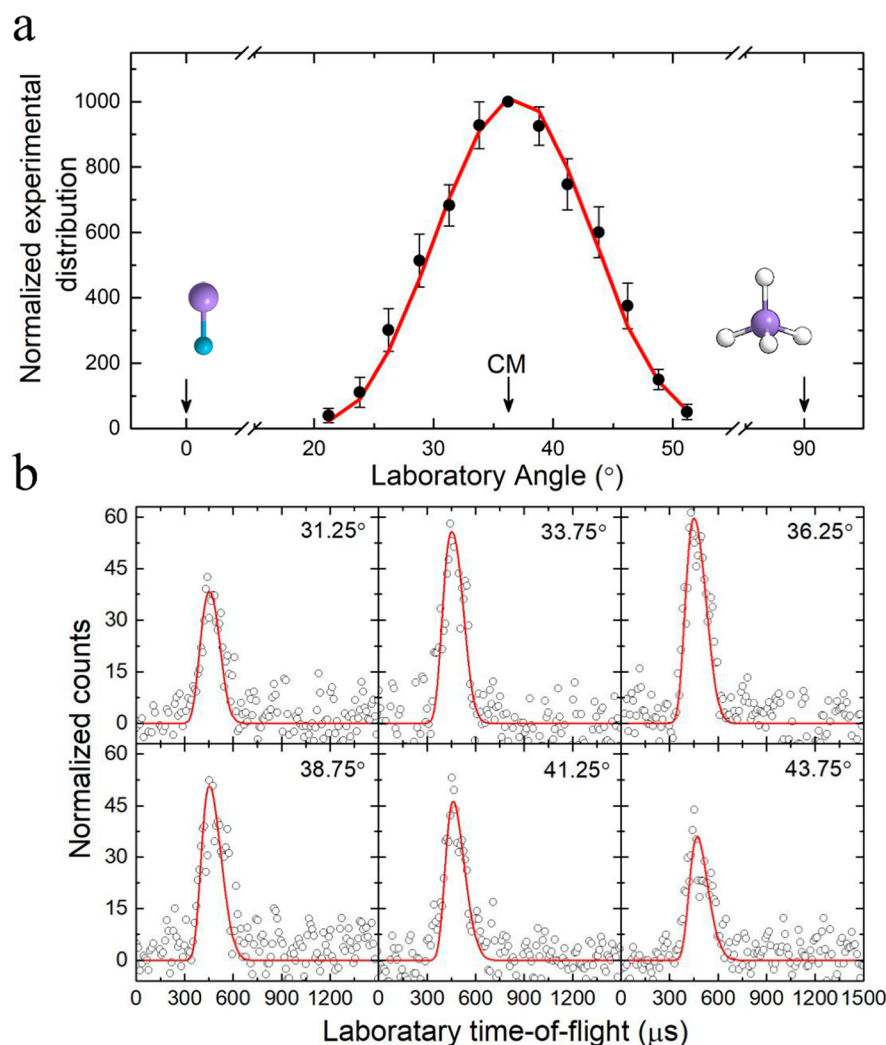


**Figure 1.** Laboratory angular distribution (a) and time-of-flight spectra (b) recorded in the reaction of the D1-silylydne radical with silane at mass-to-charge ratio of  $m/z = 61$ . The solid circles with their error bars represent the normalized experimental distribution; the open circles indicate the experimental data. The red lines represent the best fits obtained from the optimized center-of-mass (CM) functions, as depicted in Figure 2. Silicon, deuterium, and hydrogen are color coded in purple, light blue, and white, respectively.

rotating silicon rod with 4–8 mJ, 266 nm pulses (Spectra-Physics Quanta-Ray Pro 270 Nd:YAG laser; 30 Hz) in the primary chamber and entrainment of the ablated species in a 1:1 mixture of deuterium gas ( $D_2$ , 99.7%; Icon Isotopes, Inc.) and neon (Ne, 99.999%; Specialty Gases of America) with 4 atm total pressure. Due to the natural silicon isotope abundances ( $^{28}\text{Si}$  (92.2%),  $^{29}\text{Si}$  (4.7%),  $^{30}\text{Si}$  (3.1%)), the D1-silylydne beam was optimized at  $m/z = 31$  for intensity. This mass-to-charge value is unique to the D1-silylydne radical. The D1-silylydne beam was first collimated by a skimmer and then velocity selected by chopper wheel ( $2083.3 \pm 0.1 \mu\text{s}$ ), which is controlled by a precision motion system (motor, 2057S024B, Faulhaber; controller, MC 5005 S RS, Faulhaber). Cables used for the motion system need to be shielded to ensure an interference-free environment. Finally, the peak velocity ( $v_p$ ) and speed ratio ( $S$ ) of the D1-silylydne beam were  $1206 \pm 25 \text{ m s}^{-1}$  and  $6.1 \pm 1.1$ , respectively. In the selected part of the beam, a D1-silylydne to atomic silicon ratio of  $0.12 \pm 0.02:1$  was determined, i.e., a fraction of about 10%. No higher molecular weight silicon–deuterium bearing species were present in the primary beam under the experimental conditions. Notice that even if D1-silylydne

radicals in the  $A^2\Delta$  state are formed initially, considering about  $18 \mu\text{s}$  travel time to the interaction region of our scattering chamber and  $500 \text{ ns}$   $A^2\Delta$  lifetime,<sup>35</sup> any electronically excited radical will decay to the ground state. In the interaction region, the supersonic beam of pure silane (Linde; 99.999%) with  $v_p$  of  $827 \pm 20 \text{ m s}^{-1}$  and  $S$  of  $10.1 \pm 0.2$  crossed perpendicularly with the primary D1-silylydne beam. The center-of mass (CM) angle and collision energy of this reaction are then determined to  $16.6 \pm 0.5 \text{ kJ mol}^{-1}$  and  $36.2 \pm 0.6^\circ$ , respectively (Table S1). Both primary and secondary supersonic beams were operated at 60 Hz and a 30 Hz laser was used for the ablation; thus, potential background counts can be eliminated by the laser-on minus laser-off method.

Our scattering experiment was conducted exploiting a quadrupole mass spectrometer (QMS); the products were ionized with an electron impact ionizer at 80 eV which is housed in an ultrahigh vacuum chamber at a pressure of  $7 \times 10^{-12}$  Torr.<sup>36,37</sup> Ions are then filtered according to their distinct mass-to-charge ratios ( $m/z$ ) and recorded by a Daly type detector. In order to record angular-resolved TOF spectra, the detector assembly is designed to be rotatable within the plane defined by the primary and secondary supersonic beams. By

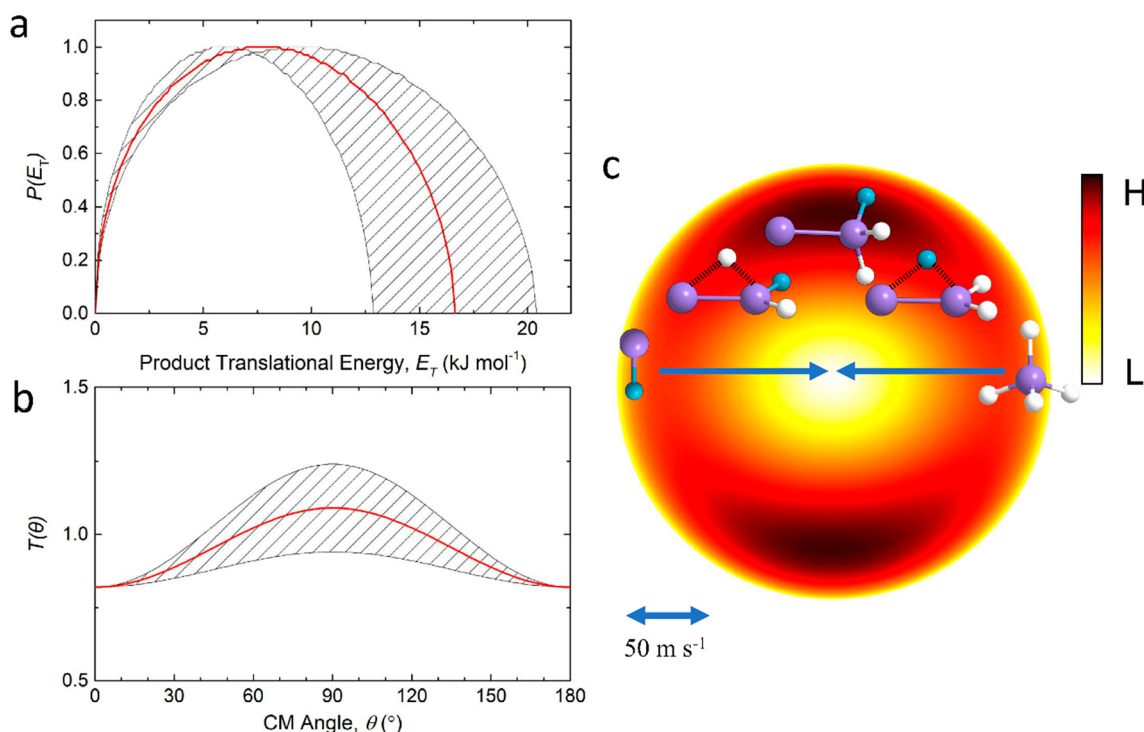


**Figure 2.** Center-of-mass (CM) translational energy flux distribution (a), angular distribution (b), and the corresponding flux contour map (c) for the reaction of D1-silyldiyne with silane. Shaded areas indicate the error limits of the best fits; the red solid lines define the best-fit functions. The flux contour map symbolizes the reactive scattering products as a function of the CM scattering angle ( $\theta$ ) and product velocity ( $u$ ). The color bar indicates the flux gradient from high (H) intensity to low (L) intensity. Silicon, deuterium, and hydrogen are color coded in purple, light blue, and white, respectively.

use of a forward-convolution routine based on the Jacobian transformation,<sup>38,39</sup> the collected laboratory data were transformed into the CM reference frame for the scattering dynamics information. As a result, in the CM system, angular  $T(\theta)$  and translational energy  $P(E_T)$  flux distributions can be derived. Meanwhile, in the lab system, the angular distributions and laboratory TOF spectra are also reconstructed from the optimized  $T(\theta)$  and  $P(E_T)$  functions. The reactive differential cross section  $I(u, \theta) \approx P(u) \times T(\theta)$  is extracted from these functions and can be seen as an overall image of the reaction dynamics.<sup>40,41</sup>

**2.2. Computational and Statistical Calculations.** The molecular hydrogen loss channels of the SiH + SiH<sub>4</sub> reaction on the Si<sub>2</sub>H<sub>5</sub> adiabatic doublet ground-state potential energy surface is characterized. The structures for collision complexes, intermediates due to isomerization, transition states, and H<sub>2</sub> dissociation products along the pathways are optimized by the coupled cluster<sup>42–45</sup> CCSD/cc-pVTZ calculations. The energies are further refined to CCSD(T)/CBS complete basis set limits,<sup>46</sup> with CCSD/cc-pVTZ zero-point energy corrections, by extrapolating the CCSD(T)/cc-pVDZ, CCSD(T)/cc-pVTZ, and CCSD(T)/cc-pVQZ energies. This ensures an accuracy within 7 kJ mol<sup>-1</sup>.<sup>47</sup> The corresponding potential energy surface for the SiD + SiH<sub>4</sub> reaction is then obtained by substituting D-corrected zero-point energies. GAUSSIAN16 programs<sup>48</sup> are employed in the *ab initio* electronic structure calculations.

The energy dependent Rice–Ramsperger–Kassel–Marcus (RRKM) rate constants<sup>49</sup> for the SiD + SiH<sub>4</sub> reaction are predicted at collision energies of 8.0, 10.0, and 16.6 kJ/mol. The saddle-point method<sup>49,50</sup> is utilized to evaluate the density of the intermediate states and the number of transition states;

with the CCSD(T)/CBS energies and CCSD/cc-pVTZ harmonic frequencies, the species are calculated as a collection of harmonic oscillators. The variational transition states (tsi2p2 and its deuterated counter parts) along the barrierless paths are located with variational RRKM theory.<sup>51–53</sup> Utilizing RRKM rate constants, product (H<sub>2</sub>, HD) branching ratios are derived by solving the reaction mechanism (*ab initio* reaction paths) rate equations with the Runge–Kutta method.

### 3. RESULTS

**3.1. Laboratory Frame.** For the crossed molecular beam experiments of the D1-silyldiyne radical (SiD; X<sup>2</sup>Π) with silane (SiH<sub>4</sub>; X<sup>1</sup>A<sub>1</sub>), we must account first for the natural silicon isotope abundances [<sup>28</sup>Si (92.2%), <sup>29</sup>Si (4.7%), <sup>30</sup>Si (3.1%)] for both reactants. This might complicate the elucidation if the laboratory data originate from the atomic and/or molecular hydrogen loss. However, considering the collision energy of 16.6 ± 0.5 kJ mol<sup>-1</sup> under our experimental conditions, electronic structure calculations reveal (Section 4, Discussion) that it is energetically not feasible to form even the thermodynamically most stable Si<sub>2</sub>H<sub>4</sub> isomer along with atomic hydrogen since this channel is endoergic by 86 kJ mol<sup>-1</sup>. The atomic hydrogen (deuterium) loss channels are therefore closed, and only the molecular hydrogen (H<sub>2</sub>) and/or hydrogen deuteride (HD) loss channels are energetically accessible. Second, besides the D1-silyldiyne radical, the primary beam also contains ground state atomic silicon Si(<sup>3</sup>P<sub>j</sub>), which reacts with silane to form Si<sub>2</sub>H<sub>2</sub> isomers plus molecular hydrogen as well; the atomic hydrogen loss channel in the Si–SiH<sub>4</sub> system is endoergic (+137 kJ mol<sup>-1</sup>) and therefore is closed.<sup>54</sup> Recall that for ref 54, the reactive scattering signal was collected from  $m/z = 60$  to 58 with signals at  $m/z = 59$

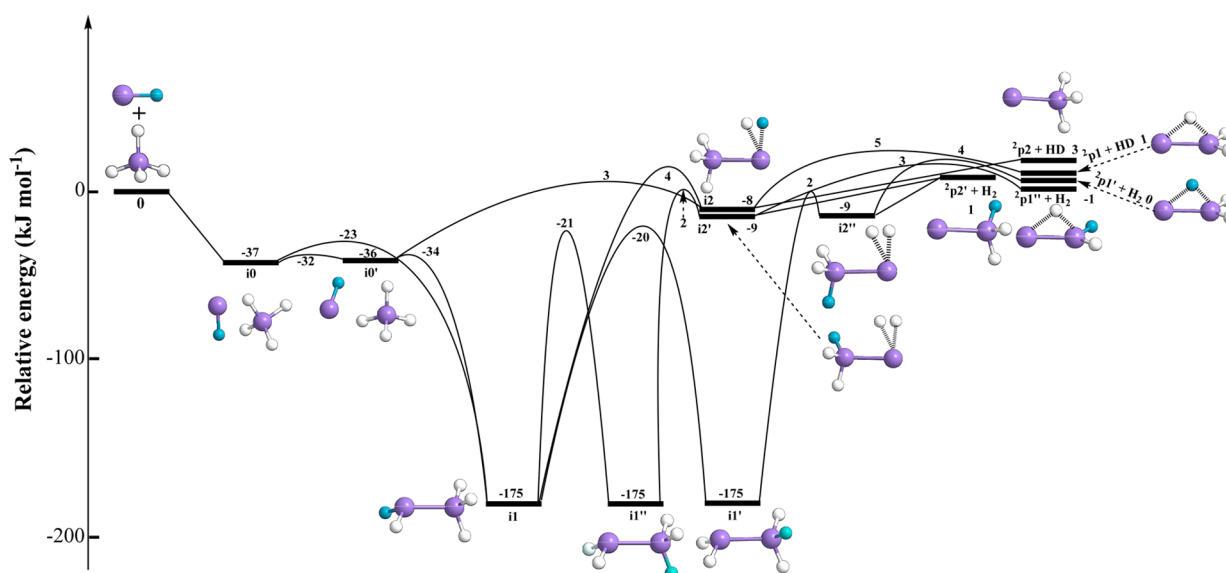


**Figure 3.** CCSD/cc-pVTZ//CCSD(T)/CBS potential energy surface for the reaction of the D1-silylydne radical with silane including molecular hydrogen and hydrogen deuteride loss pathways. A complete potential energy surface including all the  $\text{Si}_2\text{H}_3$  isomers for the reaction of silylydne with silane is presented in Figure S3. Silicon, hydrogen, and deuterium are color coded in purple, white, and light blue, respectively. Optimized geometries are compiled in Tables S4 and S8.

and 60 recorded at levels of  $(7.0 \pm 0.3)\%$  and  $(13.2 \pm 0.7)\%$  compared to  $m/z = 58$  (Table S3). It shall be stressed that no signal at  $m/z = 61$  is detectable in the Si–SiH<sub>4</sub> system.

The reactive scattering signal was explored from mass-to-charge ( $m/z$ ) 64 to 58 (Supporting Information; Tables S2 and S3). No reactive scattering signal could be detected from  $m/z = 64$  to 62 but only from  $m/z = 61$  to 58. Therefore, we can conclude that only the signal at  $m/z = 61$  is unique to the SiD–SiH<sub>4</sub> system since ion counts at lower  $m/z$  values were also observed in the Si–SiH<sub>4</sub> system. Consequently, angular resolved TOF spectra were collected at  $m/z = 61$ ; the resulting laboratory angular distribution was spread about  $30^\circ$  (Figure 1). The nearly forward–backward symmetry of the angular distribution and the CM angle of  $36.2 \pm 0.6^\circ$  suggests indirect scattering dynamics by forming Si<sub>2</sub>DH<sub>4</sub> complex(es).<sup>40</sup> Here, signal at  $m/z = 61$  can originate from ionized <sup>28</sup>Si<sup>29</sup>SiH<sub>2</sub>D, <sup>29</sup>Si<sub>2</sub>H<sub>3</sub>, and/or <sup>28</sup>Si<sup>30</sup>SiH<sub>3</sub> (Table S2). These findings suggest that the molecular hydrogen (H<sub>2</sub>) and/or the hydrogen deuteride (HD) loss channels are open in the SiD–SiH<sub>4</sub> system along with the formation of Si<sub>2</sub>H<sub>2</sub>D and/or Si<sub>2</sub>H<sub>3</sub> species, respectively.

**3.2. Center-of-Mass Frame.** With a single-channel-fit through the reaction of <sup>29</sup>SiD (31 amu) plus <sup>28</sup>SiH<sub>4</sub> (32 amu) along with the mass combination of the products of 61 amu (<sup>28</sup>Si<sup>29</sup>SiDH<sub>2</sub>) and 2 amu (H<sub>2</sub>) (Figures 1 and 2), the laboratory data could be replicated, and the information in the CM reference frame on the reaction dynamics is obtained.<sup>40</sup> Considering the natural isotopes, a single-channel-fit was also accomplished for the <sup>28</sup>SiD plus <sup>29</sup>SiH<sub>4</sub> reactants yielding products of 61 amu (<sup>28</sup>Si<sup>29</sup>SiDH<sub>2</sub>; hereafter: Si<sub>2</sub>DH<sub>2</sub>) and 2 amu (H<sub>2</sub>) (Figures S1 and S2) utilizing essentially identical CM functions. Most important, the laboratory data could also account for the <sup>30</sup>SiD plus <sup>28</sup>SiH<sub>4</sub> and <sup>28</sup>SiD plus <sup>30</sup>SiH<sub>4</sub> reactions yielding in both cases <sup>28</sup>Si<sup>30</sup>SiH<sub>3</sub> (hereafter: Si<sub>2</sub>H<sub>3</sub>) plus hydrogen deuteride (HD) (Figures S1 and S2); these CM functions are nearly identical with those of the <sup>29</sup>SiH plus <sup>28</sup>SiH<sub>4</sub> and <sup>28</sup>SiH plus <sup>29</sup>SiH<sub>4</sub> systems. Consequently, the

laboratory data can be replicated with both the Si<sub>2</sub>H<sub>3</sub> + HD and the Si<sub>2</sub>DH<sub>2</sub> + H<sub>2</sub> channels.

The nature of the product isomer(s) can be revealed through the analysis of the CM translational energy distribution  $P(E_T)$ . For the D1-silylydne–silane system, for those molecules without internal excitation, the reaction exoergicity can be obtained by subtracting the collision energy ( $16.6 \pm 0.5 \text{ kJ mol}^{-1}$ ) from the maximum translational energy  $E_{\text{max}}$  ( $17 \pm 5 \text{ kJ mol}^{-1}$ ); this results in a thermoneutral reaction of  $0 \pm 5 \text{ kJ mol}^{-1}$ .<sup>40</sup> Furthermore, a rather loose exit transition state is suggested with the maximum of the  $P(E_T)$  distribution of  $5\text{--}10 \text{ kJ mol}^{-1}$ , leading to the formation of Si<sub>2</sub>H<sub>3</sub> and/or Si<sub>2</sub>DH<sub>2</sub> from the Si<sub>2</sub>DH<sub>4</sub> intermediate(s). Finally, a forward–backward symmetric CM angular distribution  $T(\theta)$  shows a maximum at  $90^\circ$  and intensity over the complete scattering range. These findings support indirect (complex forming) reaction mechanisms via long-lived intermediates whose lifetimes are longer than, or at least competitive with, their rotational periods.<sup>40,55</sup> The distribution maximum at  $90^\circ$  reveals that the molecular hydrogen/hydrogen deuteride emits nearly parallel to the total angular momentum vector and almost perpendicularly to the rotational plane of the fragmenting intermediate, indicating significant geometrical constraints in the exit channel.<sup>40,55</sup>

#### 4. DISCUSSION

To unravel the formation of the isomers and the underlying reaction mechanism(s), we are now merging the experimental data with electronic structure calculations. The accuracy of the relative energies of the local minima, transition states, and reaction energies is within  $7 \text{ kJ mol}^{-1}$ . As revealed in Figures 3 and S3, the formation of <sup>2</sup>p<sub>4</sub> and <sup>2</sup>p<sub>6</sub> is endoergic by 18 and 66  $\text{kJ mol}^{-1}$ , respectively. Therefore, these channels are closed considering the experimental collision energy of  $16.6 \text{ kJ mol}^{-1}$ . The formation of the disilynyl (<sup>2</sup>p<sub>3</sub>; H<sub>2</sub>SiSiH; X<sup>2</sup>A;  $\Delta_R G = 4 \pm 4 \text{ kJ mol}^{-1}$ ) product can also be excluded since it can only be formed via tight exit transition states lying at least  $35 \text{ kJ mol}^{-1}$  above the separated reactants. However, the formation of

monobridged silyldynesilylene [ $\text{Si}(\mu\text{-D})\text{SiH}_2$ ,  $\text{Si}(\mu\text{-H})\text{SiHD}$ ,  $\text{Si}(\mu\text{-H})\text{SiH}_2$ ;  ${}^2\text{p1}$ ,  ${}^2\text{p1}'$ ,  ${}^2\text{p1}''$ ] and silylsilyldyne [ $\text{H}_3\text{SiSi}$ ,  $\text{H}_2\text{DSiSi}$ ;  ${}^2\text{p2}$ ,  ${}^2\text{p2}'$ ] is energetically feasible considering reaction energies of  $-1 \pm 7$  to  $1 \pm 7$   $\text{kJ mol}^{-1}$  and  $1 \pm 7$  to  $3 \pm 7$   $\text{kJ mol}^{-1}$ , respectively.

How are these potential products formed? To simplify the PES, all transition states and products higher than 16.6  $\text{kJ mol}^{-1}$  (our experimental collision energy) have been removed. As shown in the potential energy surface (PES), the reaction begins with the formation of a weakly bound van-der-Waals complex  $\text{i0}$  ( $X^2A''$ ) lying 37  $\text{kJ mol}^{-1}$  below the separated reactants. This complex can isomerize to the van-der-Waals complex  $\text{i0}'$  ( $X^2A$ ) by rotation of the SiD radical residing 36  $\text{kJ mol}^{-1}$  below the separated reactants or rearranges by inserting the SiD radical into the silicon–hydrogen single bonds of silane involving a barrier of 14  $\text{kJ mol}^{-1}$  leading to the D1-silylsilyl radical ( $\text{HDSiSiH}_3$ ,  $\text{i1}$ ,  $X^2A'$ ). This reaction is effectively barrier-less since the barrier is submerged and below the separated reactants. Intermediates  $\text{i0}'$  and  $\text{i1}$  are also connected via a barrier of only 2  $\text{kJ mol}^{-1}$  above  $\text{i0}'$ . A hydrogen migration isomerizes  $\text{i1}$  to  $\text{i1}''$  ( $\text{H}_2\text{SiSiDH}_2$ ,  $X^2A'$ ) or  $\text{i1}'$  ( $\text{H}_2\text{SiSiHDH}$ ,  $X^2A'$ ). Intermediates  $\text{i2}$  ( $\text{HDSiSiH}_3$ ,  $X^2A''$ ),  $\text{i2}'$  ( $\text{H}_2\text{SiSiHDH}$ ,  $X^2A''$ ), and  $\text{i2}''$  ( $\text{H}_2\text{SiSiDH}_2$ ,  $X^2A''$ ) are nearly isoenergetic and can be accessed from  $\text{i1}$ ,  $\text{i1}''$ , and  $\text{i1}'$  via barriers of 179, 177, and 177  $\text{kJ mol}^{-1}$ , respectively. The van-der-Waals complex  $\text{i0}'$  can also isomerize to intermediate  $\text{i2}$  via a barrier of 39  $\text{kJ mol}^{-1}$ . Finally, all five products in Figure 3 are nearly isoenergetic depicting slightly exoergic ( $-1$   $\text{kJ mol}^{-1}$ ) to endoergic (3  $\text{kJ mol}^{-1}$ ) reaction; these products can be formed via  $\text{H}_2$  or HD loss ( ${}^2\text{p1}$  ( $\text{Si}(\text{H})\text{SiH}_2$ ;  $X^2A''$ ),  ${}^2\text{p1}''$  ( $\text{Si}(\text{H})\text{SiDH}$ ;  $X^2A$ ),  ${}^2\text{p1}'$  ( $\text{Si}(\text{D})\text{SiH}_2$ ;  $X^2A''$ ),  ${}^2\text{p2}$  ( $\text{H}_3\text{SiSi}$ ;  $X^2A$ ),  ${}^2\text{p2}'$  ( $\text{H}_2\text{DSiSi}$ ;  $X^2A$ )). Among these products,  ${}^2\text{p2}$  is formed from  $\text{i2}$  via a barrierless HD elimination;  $\text{i2}'$  and  $\text{i2}''$  are found to undergo barrierless unimolecular decomposition via molecular hydrogen loss to the same product  ${}^2\text{p2}'$ . As for the remaining possible products, the unimolecular decomposition of  $\text{i2}$  can lead to the monobridged isomer  ${}^2\text{p1}$  plus HD via a barrier of 13  $\text{kJ mol}^{-1}$ ;  ${}^2\text{p1}''$  and  ${}^2\text{p1}'$  along with molecular hydrogen are formed from intermediates  $\text{i2}'$  and  $\text{i2}''$  after passing barriers of 12 and 13  $\text{kJ mol}^{-1}$ , respectively. Likewise, the loose exit transition state leading to the formation of  ${}^2\text{p1}'$ ,  ${}^2\text{p1}''$ , and  ${}^2\text{p1}$  lies only 4  $\text{kJ mol}^{-1}$  above the separated products. The statistical yields of the five products were also explored using Rice–Ramsperger–Kassel–Marcus (RRKM) theory (Table S7) revealing the branching ratios of  ${}^2\text{p1}$ ,  ${}^2\text{p2}$ ,  ${}^2\text{p1}''$ ,  ${}^2\text{p1}'$ , and  ${}^2\text{p2}'$  of 9.9%, 17.8%, 24.6%, 15.1%, and 32.7%, respectively, i.e., totaling nearly equal fractions of (partially deuterated) silyldynesilylene ( ${}^2\text{p1}$ ) and silylsilyldyne ( ${}^2\text{p2}$ ) species. These data also suggest that if the reaction is statistically, the molecular hydrogen loss channel represents the predominant channel (72.4%) with the contribution of 27.6% from hydrogen deuteride (HD) elimination.

## 5. CONCLUSION

In conclusion, combining our laboratory data with electronic structure calculations, our study exposed the molecular hydrogen ( $\text{H}_2$ /HD) loss channels via the bimolecular gas phase reaction of the D1-silyldyne radical with silane leading to the formation of monobridged silyldynesilylene [ $\text{Si}(\mu\text{-D})\text{SiH}_2$ ,  $\text{Si}(\mu\text{-H})\text{SiHD}$ ,  $\text{Si}(\mu\text{-H})\text{SiH}_2$ ] and silylsilyldyne [ $\text{H}_3\text{SiSi}$ ,  $\text{H}_2\text{DSiSi}$ ]. The indirect scattering dynamics are

initiated by forming a van-der-Waals complex  $\text{i0}$ , which can isomerize to van-der-Waals complex  $\text{i0}'$  and/or to D1-silylsilyl radical ( $\text{HDSiSiH}_3$ ,  $\text{i1}$ ,  $X^2A'$ ) by inserting the silyldyne radical into a silicon–hydrogen bond of silane; note that the latter can also be accessed via isomerization of  $\text{i0}'$ . Nearly isoenergetic hydrogen/deuterium shifts to  $\text{i1}''/\text{i1}'$  and  $\text{i2}/\text{i2}'/\text{i2}''$  may undergo molecular hydrogen loss involving loose exit transition state in nearly thermoneutral reactions ( $-1$  to  $+3 \pm 7$   $\text{kJ mol}^{-1}$ ).

It is educational to compare these dynamics within the main group XIV isovalent  $\text{EH-EH}_4$  systems ( $\text{E} = \text{C}, \text{Si}, \text{Ge}$ ). For the carbon system ( $\text{CH-CH}_4$ ), the ethyl radical intermediate ( $\text{C}_2\text{H}_5$ ,  $X^2A'$ ) is formed by inserting methylidyne into a carbon–hydrogen bond of methane. This insertion process is also barrierless, and the ethyl radical is isovalent to the silylsilyl ( $\text{H}_2\text{SiSiH}_3$ ,  $X^2A'$ ). For the  $\text{CH-CH}_4$  reaction, the atomic hydrogen loss channel is open leading to the formation of the ethylene molecule ( $\text{C}_2\text{H}_4$ ;  $X^1A_{1g}$ ) through a tight exit transition state; meanwhile the molecular hydrogen loss channel is closed.<sup>56–58</sup> The dynamics of the  $\text{SiD-SiH}_4$  system are quite distinct from this isovalent carbon system, revealing that the insight from reactivity of carbon system is not readily leveraged to interpret analogous system with the “heavier” main group XIV atoms. Detailed experimental scattering results merged with electron structure calculations represent the crucial method to elucidate the largely unexplored chemistry about silicon analogues of their hydrocarbon counterparts. The formation of the small silicon hydrides including hydrogen-bridged nonclassical transients via the elementary reaction contributes to our understanding of the main group XIV.

## ■ ASSOCIATED CONTENT

### Supporting Information

The Supporting Information is available free of charge at <https://pubs.acs.org/doi/10.1021/acs.jpca.0c11538>.

Complete potential energy surface (Figure S3), the other three possible reaction channels including the reactions of  ${}^{28}\text{SiD}$  plus  ${}^{29}\text{SiH}_4$  leading to  ${}^{28}\text{Si}^{29}\text{SiDH}_2$  plus molecular hydrogen ( $\text{H}_2$ ) and  ${}^{30}\text{SiD}$  plus  ${}^{28}\text{SiH}_4$ ,  ${}^{28}\text{SiD}$  plus  ${}^{30}\text{SiH}_4$  leading to  ${}^{28}\text{Si}^{30}\text{SiH}_3$  plus hydrogen deuteride (HD) (Figures S1 and S2), the experimental parameters and all the possible dissociation products considering the isotopes of silicon (Tables S1–S3), and Cartesian coordinates, RRKM rate constants, reaction mechanism, branching ratios, and energies on the adiabatic doublet ground state potential energy surface (Tables S4–S11) (PDF)

## ■ AUTHOR INFORMATION

### Corresponding Authors

Ralf I. Kaiser – Department of Chemistry, University of Hawai'i at Manoa, Honolulu, Hawaii 96822, United States; [orcid.org/0000-0002-7233-7206](https://orcid.org/0000-0002-7233-7206); Email: [ralfk@hawaii.edu](mailto:ralfk@hawaii.edu)

Agnes H. H. Chang – Department of Chemistry, National Dong Hwa University, Shoufeng, Hualien 974, Taiwan; Email: [hhchang@gms.ndhu.edu.tw](mailto:hhchang@gms.ndhu.edu.tw)

### Authors

Zhenghai Yang – Department of Chemistry, University of Hawai'i at Manoa, Honolulu, Hawaii 96822, United States

Bing-Jian Sun – Department of Chemistry, National Dong Hwa University, Shoufeng, Hualien 974, Taiwan

Chao He – Department of Chemistry, University of Hawai'i at Manoa, Honolulu, Hawaii 96822, United States

Shane Goettl – Department of Chemistry, University of Hawai'i at Manoa, Honolulu, Hawaii 96822, United States

Yu-Ting Lin – Department of Chemistry, National Dong Hwa University, Shoufeng, Hualien 974, Taiwan

Complete contact information is available at:  
<https://pubs.acs.org/10.1021/acs.jpca.0c11538>

### Author Contributions

<sup>§</sup>Z.Y. and B.-J.S. contributed equally to this work.

### Notes

The authors declare no competing financial interest.

## ACKNOWLEDGMENTS

The experimental work was supported by the U.S. National Science Foundation (NSF) under Award CHE-1853541. The calculations were performed with computer resources at the National Center for High-Performance Computing of Taiwan.

## REFERENCES

- (1) Langmuir, I. Isomorphism, Isosterism and Covalence. *J. Am. Chem. Soc.* **1919**, *41*, 1543–1559.
- (2) Langmuir, I. The Arrangement of Electrons in Atoms and Molecules. *J. Am. Chem. Soc.* **1919**, *41*, 868–934.
- (3) Nielsen, I. M.; Janssen, C. L.; Burton, N. A.; Schaefer, H. F., III. (1, 2)-Hydrogen Shift in Monovalent Carbon Compounds: the Methylcarbyne-Vinyl Radical Isomerization. *J. Phys. Chem.* **1992**, *96*, 2490–2494.
- (4) Wang, J.-H.; Chang, H.-C.; Chen, Y.-T. Theoretical Study of Isomeric Structures and Low-Lying Electronic States of the Vinyl Radical C<sub>2</sub>H<sub>3</sub>. *Chem. Phys.* **1996**, *206*, 43–56.
- (5) Bennett, C. J.; Jamieson, C. S.; Osamura, Y.; Kaiser, R. I. Laboratory Studies on the Irradiation of Methane in Interstellar, Cometary, and Solar System Ices. *Astrophys. J.* **2006**, *653*, 792.
- (6) Kaiser, R. I.; Osamura, Y. Laboratory Studies on the Infrared Absorptions of Hydrogenated Carbon-Silicon Clusters: Directing the Identification of Organometallic SiCH<sub>x</sub> Species toward IRC + 10216. *Astrophys. J.* **2005**, *630*, 1217.
- (7) Yang, Z.; Doddipatla, S.; Kaiser, R. I.; Krasnoukhov, V. S.; Azyazov, V. N.; Mebel, A. M. Directed Gas Phase Formation of the Elusive Silylgermylidene Radical (H<sub>3</sub>SiGe, X<sub>2</sub>A<sup>+</sup>). *ChemPhysChem* **2021**, *22*, 184–191.
- (8) Yang, Z.; He, C.; Doddipatla, S.; Krasnoukhov, V. S.; Azyazov, V. N.; Mebel, A. M.; Kaiser, R. I. Gas Phase Formation of Methylgermylene (HGeCH<sub>3</sub>). *ChemPhysChem* **2020**, *21*, 1898–1904.
- (9) Thomas, A. M.; Dangi, B. B.; Yang, T.; Tarczay, G.; Kaiser, R. I.; Sun, B.-J.; Chen, S.-Y.; Chang, A. H.; Nguyen, T. L.; Stanton, J. F.; et al. Directed Gas-Phase Formation of the Germaniumsilylene Butterfly Molecule (Ge(μ-H<sub>2</sub>)Si). *J. Phys. Chem. Lett.* **2019**, *10*, 1264–1271.
- (10) Carrier, W.; Zheng, W.; Osamura, Y.; Kaiser, R. I. Infrared Spectroscopic Identification of Digermene, Ge<sub>2</sub>H<sub>4</sub> (X<sup>1</sup>A<sub>g</sub>), and of the Digermeryl Radical, Ge<sub>2</sub>H<sub>3</sub> (X<sup>2</sup>A<sup>+</sup>), together with their Deuterated Counterparts in Low Temperature Germane Matrices. *Chem. Phys.* **2006**, *330*, 275–286.
- (11) Li, Q. S.; Lü, R. H.; Xie, Y.; Schaefer, H. F., III Molecules for Materials: Germanium Hydride Neutrals and Anions. Molecular Structures, Electron Affinities, and Thermochemistry of GeH<sub>n</sub>/GeH<sub>n</sub><sup>-</sup> (n = 0–4) and Ge<sub>2</sub>H<sub>n</sub>/Ge<sub>2</sub>H<sub>n</sub><sup>-</sup> (n = 0–6). *J. Comput. Chem.* **2002**, *23*, 1642–1655.
- (12) Ricca, A.; Bauschlicher, C. W. Heats of Formation for GeH<sub>n</sub> (n = 1–4) and Ge<sub>2</sub>H<sub>n</sub> (n = 1–6). *J. Phys. Chem. A* **1999**, *103*, 11121–11125.
- (13) Curtiss, L. A.; Raghavachari, K.; Deutsch, P. W.; Pople, J. A. Theoretical Study of Si<sub>2</sub>H<sub>n</sub> (n = 0–6) and Si<sub>2</sub>H<sub>n</sub><sup>+</sup> (n = 0–7): Appearance Potentials, Ionization Potentials, and Enthalpies of Formation. *J. Chem. Phys.* **1991**, *95*, 2433–2444.
- (14) Sax, A. F.; Kalcher, J. Theoretical Enthalpies of Formation for Small Silicon Hydrides. *J. Phys. Chem.* **1991**, *95*, 1768–1783.
- (15) Gong, X. G.; Guenzburger, D.; Saitovitch, E. B. Structure and Dynamic Properties of Neutral and Ionized SiH<sub>5</sub> and Si<sub>2</sub>H<sub>3</sub>. *Chem. Phys. Lett.* **1997**, *275*, 392–398.
- (16) Choukri, H.; Guermoune, A.; Schmitzer, A. R.; Villemin, D.; Cherqaoui, D.; Jarid, A. DFT and CCSD(T) Study of the Disilicon Trihydride (Si<sub>2</sub>H<sub>3</sub>) Isomerization, Unprecedented Isomeric Structures. *J. Mol. Struct.: THEOCHEM* **2008**, *852*, 30–35.
- (17) Ernst, M.; Sax, A.; Kalcher, J. Intramolecular H-transfer Reactions in Si<sub>2</sub>H<sub>n</sub> (for n = 3–5). *Chem. Phys. Lett.* **1993**, *216*, 189–193.
- (18) Sari, L.; McCarthy, M.; Schaefer, H. F.; Thaddeus, P. Mono- and Dibriged Isomers of Si<sub>2</sub>H<sub>3</sub> and Si<sub>2</sub>H<sub>4</sub>: the True Ground State Global Minima. Theory and Experiment in Concert. *J. Am. Chem. Soc.* **2003**, *125*, 11409–11417.
- (19) Pak, C.; Rienstra-Kiracofe, J. C.; Schaefer, H. F. Electron Affinities of Silicon Hydrides: SiH<sub>n</sub> (n = 0–4) and Si<sub>2</sub>H<sub>n</sub> (n = 0–6). *J. Phys. Chem. A* **2000**, *104*, 11232–11242.
- (20) Purnell, J.-H.; Walsh, R. The Pyrolysis of Monosilane. *Proc. R. Soc. London, Ser. A* **1966**, *293*, 543–561.
- (21) Ring, M. A.; O'Neal, H. E. Mechanism of the Thermally Induced Gas-Phase Decomposition of Silane: A Revisitation. *J. Phys. Chem.* **1992**, *96*, 10848–10855.
- (22) Newman, C. G.; Ring, M. A.; O'Neal, H. E. Kinetics of the Silane and Silylene Decompositions under Shock Tube Conditions. *J. Am. Chem. Soc.* **1978**, *100*, 5945–5946.
- (23) Tonokura, K.; Murasaki, T.; Koshi, M. Formation Mechanism of Hydrogenated Silicon Clusters during Thermal Decomposition of Disilane. *J. Phys. Chem. B* **2002**, *106*, 555–563.
- (24) Gupte, G. R.; Prasad, R. Ground State Geometries and Vibrational Spectra of Small Hydrogenated Silicon Clusters using Nonorthogonal Tight-Binding Molecular Dynamics. *Int. J. Mod. Phys. B* **1998**, *12*, 1607–1622.
- (25) Ruscic, B.; Berkowitz, J. Photoionization Mass Spectrometric Studies of the Transient Species Si<sub>2</sub>H<sub>n</sub> (n = 2–5). *J. Chem. Phys.* **1991**, *95*, 2416–2432.
- (26) Sillars, D.; Bennett, C. J.; Osamura, Y.; Kaiser, R. I. Infrared Spectroscopic Detection of the Disilylenyl (Si<sub>2</sub>H<sub>3</sub>) and d3-Disilylenyl (Si<sub>2</sub>D<sub>3</sub>) Radicals in Silane and d4-Silane Matrices. *Chem. Phys. Lett.* **2004**, *392*, 541–548.
- (27) Kaiser, R.; Osamura, Y. Infrared Spectroscopic Studies of Hydrogenated Silicon Clusters—Guiding the Search for Si<sub>2</sub>H<sub>x</sub> Species in the Circumstellar Envelope of IRC+10216. *Astron. Astrophys.* **2005**, *432*, 559–566.
- (28) Begemann, M.; Dreyfus, R.; Jasinski, J. Absolute Rate Constants for the Reaction of SiH with Hydrogen, Deuterium and Silane. *Chem. Phys. Lett.* **1989**, *155*, 351–355.
- (29) Nemoto, M.; Suzuki, A.; Nakamura, H.; Shibuya, K.; Obi, K. Electronic Quenching and Chemical Reactions of SiH Radicals in the Gas Phase. *Chem. Phys. Lett.* **1989**, *162*, 467–471.
- (30) Nomura, H.; Akimoto, K.; Kono, A.; Goto, T. Rate Constants for the Reactions of SiH and SiH<sub>2</sub> with SiH<sub>4</sub> in a Low-Pressure SiH<sub>4</sub> Plasma. *J. Phys. D: Appl. Phys.* **1995**, *28*, 1977.
- (31) Kaiser, R. I.; Maksyutenko, P.; Ennis, C.; Zhang, F.; Gu, X.; Krishtal, S. P.; Mebel, A. M.; Kostko, O.; Ahmed, M. Untangling the Chemical Evolution of Titan's Atmosphere and Surface—From Homogeneous to Heterogeneous Chemistry. *Faraday Discuss.* **2010**, *147*, 429–478.
- (32) Mebel, A. M.; Kaiser, R. I. Formation of Resonantly Stabilised Free Radicals via the Reactions of Atomic Carbon, Dicarbon, and Tricarbon with Unsaturated Hydrocarbons: Theory and Crossed Molecular Beams Experiments. *Int. Rev. Phys. Chem.* **2015**, *34*, 461–514.

- (33) Yang, T.; Thomas, A. M.; Dangi, B. B.; Kaiser, R. I.; Mebel, A. M.; Millar, T. J. Directed Gas Phase Formation of Silicon Dioxide and Implications for the Formation of Interstellar Silicates. *Nat. Commun.* **2018**, *9*, 774.
- (34) Parker, D. S.; Wilson, A. V.; Kaiser, R. I.; Mayhall, N. J.; Head-Gordon, M.; Tielens, A. G. On the Formation of Silacyclopropenyldiene ( $c\text{-SiC}_2\text{H}_2$ ) and its Role in the Organosilicon Chemistry in the Interstellar Medium. *Astrophys. J.* **2013**, *770*, 33.
- (35) Bauer, W.; Becker, K. H.; Düren, R.; Hubrich, C.; Meuser, R. Radiative Lifetime Measurements of SiH ( $A^2\Delta$ ) by Laser-Induced Fluorescence. *Chem. Phys. Lett.* **1984**, *108*, 560–561.
- (36) Daly, N. Scintillation Type Mass Spectrometer Ion Detector. *Rev. Sci. Instrum.* **1960**, *31*, 264–267.
- (37) Brink, G. O. Electron Bombardment Molecular Beam Detector. *Rev. Sci. Instrum.* **1966**, *37*, 857–860.
- (38) Weiss, P. S. Reaction Dynamics of Electronically Excited Alkali Atoms with Simple Molecules. Ph.D. Thesis, University of California: Berkeley, CA, 1986.
- (39) Kaiser, R. I.; Le, T. N.; Nguyen, T. L.; Mebel, A. M.; Balucani, N.; Lee, Y. T.; Stahl, F.; Schleyer, P. v. R.; Schaefer, H. F., III. A Combined Crossed Molecular Beam and Ab Initio Investigation of  $\text{C}_2$  and  $\text{C}_3$  Elementary Reactions with Unsaturated Hydrocarbons—Pathways to Hydrogen Deficient Hydrocarbon Radicals in Combustion Flames. *Faraday Discuss.* **2001**, *119*, 51–66.
- (40) Levine, R. D. *Molecular Reaction Dynamics*; Cambridge University Press: Cambridge, U.K., 2009.
- (41) Kaiser, R.; Parker, D.; Zhang, F.; Landera, A.; Kislov, V.; Mebel, A. PAH Formation under Single Collision Conditions: Reaction of Phenyl Radical and 1, 3-Butadiene to Form 1, 4-Dihydronaphthalene. *J. Phys. Chem. A* **2012**, *116*, 4248–4258.
- (42) Purvis, G. D., III; Bartlett, R. J. A Full Coupled-Cluster Singles and Doubles Model: The Inclusion of Disconnected Triples. *J. Chem. Phys.* **1982**, *76*, 1910–1918.
- (43) Hampel, C.; Peterson, K. A.; Werner, H.-J. A Comparison of the Efficiency and Accuracy of the Quadratic Configuration Interaction (QCISD), Coupled Cluster (CCSD), and Brueckner Coupled Cluster (BCCD) Methods. *Chem. Phys. Lett.* **1992**, *190*, 1–12.
- (44) Knowles, P. J.; Hampel, C.; Werner, H. J. Coupled Cluster Theory for High Spin, Open Shell Reference Wave Functions. *J. Chem. Phys.* **1993**, *99*, 5219–5227.
- (45) Deegan, M. J.; Knowles, P. J. Perturbative Corrections to Account for Triple Excitations in Closed and Open Shell Coupled Cluster Theories. *Chem. Phys. Lett.* **1994**, *227*, 321–326.
- (46) Peterson, K. A.; Woon, D. E.; Dunning, T. H., Jr Benchmark Calculations with Correlated Molecular Wave Functions. IV. The Classical Barrier Height of the  $\text{H} + \text{H}_2 \rightarrow \text{H}_2 + \text{H}$  Reaction. *J. Chem. Phys.* **1994**, *100*, 7410–7415.
- (47) Peterson, K. A.; Dunning, T. H., Jr Intrinsic Errors in Several ab Initio Methods: The Dissociation Energy of  $\text{N}_2$ . *J. Phys. Chem.* **1995**, *99*, 3898–3901.
- (48) Frisch, M.; Trucks, G.; Schlegel, H.; Scuseria, G.; Robb, M.; Cheeseman, J.; Scalmani, G.; Barone, V.; Petersson, G.; Nakatsuji, H. *Gaussian 16*, Rev. B. 01; Gaussian, Inc.: Wallingford, CT, 2016.
- (49) Chang, A. H. H.; Mebel, A. M.; Yang, X.-M.; Lin, S. H.; Lee, Y. T. Ab initio/RRKM Approach toward the Understanding of Ethylene Photodissociation. *J. Chem. Phys.* **1998**, *109*, 2748–2761.
- (50) Eyring, H.; Lin, S. H.; Lin, S. M. *Basic Chemical Kinetics*; John Wiley & Sons Inc.: New York, NY, 1980.
- (51) Hase, W. L. Variational Unimolecular Rate Theory. *Acc. Chem. Res.* **1983**, *16*, 258–264.
- (52) Marcus, R. A. On the Theory of the State Distribution of the Reaction Products and Rates of Unimolecular Dissociations. *Chem. Phys. Lett.* **1988**, *144*, 208–214.
- (53) Chang, A. H. H.; Hwang, D. W.; Yang, X.-M.; Mebel, A. M.; Lin, S. H.; Lee, Y. T. Toward the Understanding of Ethylene Photodissociation: Theoretical Study of Energy Partition in Products and Rate Constants. *J. Chem. Phys.* **1999**, *110*, 10810–10820.
- (54) Yang, T.; Dangi, B. B.; Kaiser, R. I.; Chao, K. H.; Sun, B. J.; Chang, A. H. H.; Nguyen, T. L.; Stanton, J. F. Gas-Phase Formation of the Disilavinylidene ( $\text{H}_2\text{SiSi}$ ) Transient. *Angew. Chem., Int. Ed.* **2017**, *56*, 1264–1268.
- (55) Miller, W.; Safron, S.; Herschbach, D. Exchange Reactions of Alkali Atoms with Alkali Halides: A Collision Complex Mechanism. *Discuss. Faraday Soc.* **1967**, *44*, 108–122.
- (56) Fleurat-Lessard, P.; Rayez, J.-C.; Bergeat, A.; Loison, J.-C. Reaction of Methylidyne CH ( $X^2\Pi$ ) Radical with  $\text{CH}_4$  and  $\text{H}_2\text{S}$ : Overall Rate Constant and Absolute Atomic Hydrogen Production. *Chem. Phys.* **2002**, *279*, 87–99.
- (57) Canosa, A.; Sims, I. R.; Travers, D.; Smith, I. W.; Rowe, B. Reactions of the Methylidyne Radical with  $\text{CH}_4$ ,  $\text{C}_2\text{H}_2$ ,  $\text{C}_2\text{H}_4$ ,  $\text{C}_2\text{H}_6$ , and But-1-ene Studied Between 23 and 295K with a CRESU Apparatus. *Astron. Astrophys.* **1997**, *323*, 644–651.
- (58) Ribeiro, J. M.; Mebel, A. M. Reaction Mechanism and Rate Constants of the  $\text{CH} + \text{CH}_4$  Reaction: a Theoretical Study. *Mol. Phys.* **2015**, *113*, 1865–1872.